https://doi.org/10.5194/egusphere-2026-1584
Preprint. Discussion started: 31 March 2026

Changes in groundwater-surface water interactions following two centuries of irrigation practices and groundwater use in the Upper Ganges-Yamuna interfluve, North India.

Frank J.G. van Broekhoven[1], Stefan C. Dekker[1,2], Jasper Griffioen[1,3], Anjali Bhagwat[4], Paul P. Schot[1]

[1]Copernicus Institute of Sustainable Development, Utrecht University, Utrecht, the Netherlands
[2]NIOO-KNAW, the Netherlands Institute of Ecology, Wageningen, the Netherlands
[3]TNO Geological Survey of the Netherlands, Utrecht, the Netherlands
[4]National Institute of Hydrology, Roorkee, India

Correspondence to: F.J.G. van Broekhoven (f.j.g.vanbroekhoven@uu.nl)

Short summary. Model simulations show how the water system in North-India has been altered over the past two centuries. From 1830, irrigation canals boosted recharge and raised groundwater flows to rivers and streams. After 1970, groundwater pumping, mainly for irrigation, grew sharply, lowering groundwater tables and reducing flows to surface waters. Since 2000, groundwater tables have fallen to such extent that some rivers likely lose water to the groundwater, threatening local ecosystems and drinking water.

Abstract. The Indo-Gangetic Basin (IGB) is a global hotspot for groundwater overexploitation. Previous studies have shown that groundwater levels initially rose due to enhanced recharge following the construction of irrigation canals, but subsequently declined as agricultural, municipal, and industrial abstractions intensified. However, the relative impacts of separate recharge and abstraction components (precipitation, canal leakage infiltration, irrigation return flow, and irrigation, municipal and industrial abstraction), remain unclear, as do the effects on groundwater-surface water interactions and environmental flows. This study therefore aims to quantify spatio-temporal changes in groundwater recharge and abstraction components over the past two centuries and assess how these changes have impacted groundwater–surface water interactions in the Upper Ganges–Yamuna interfluve in northern India.

Groundwater model simulations indicate that canal water infiltration following canal construction after 1830 boosted recharge, but since the 1970s increased abstractions have lowered groundwater tables and reduced river exfiltration. Currently irrigation accounts for roughly 85% of abstractions, with municipal (15%) and industrial (< 1%) uses accounting for much smaller shares. From around 2000, abstraction lowered groundwater tables to such an extent that local rivers likely shifted from draining to infiltrating conditions. As a result, groundwater–surface water interactions in local rivers may have fundamentally changed. This shift threatens environmental river flows, degrades surface water quality by limiting wastewater dilution, and harms groundwater quality where polluted river water infiltrates the aquifer, posing risks to both ecosystems and human health. Although both the Yamuna and the Ganges show reduced groundwater exfiltration, they are not (yet) infiltrating.

https://doi.org/10.5194/egusphere-2026-1584
Preprint. Discussion started: 31 March 2026

1 Introduction

Groundwater is vital for humans and ecosystems but is increasingly threatened by excessive abstractions, particularly in semi-arid irrigated areas (de Graaf et al., 2017). Groundwater depletion is widely occurring within the Indo-Gangetic Basin (IGB) making it one of the worlds hotspots of groundwater overexploitation (Gleeson et al., 2012; Marinelli et al., 2024). Satellite data from the Gravity Recovery and Climate Experiment (GRACE) reveal a steady decline in total water storage across Northern India over the past two decades (Panda et al., 2021; Rodell et al., 2009). The GRACE records since 2002 (Rodell et al., 2009), which is relatively short considering that water development in the IGB began in the 19th century with the construction of the Eastern Yamuna irrigation canal in 1830 (Irrigation and Water Resources Department, n.d.).

Long-term groundwater monitoring data offers a broader perspective. Analysis of observation wells in northwest India and central Pakistan (MacAllister et al., 2022) go back to 1900 and reveals a net increase in groundwater storage from 1900 to the 1970s. This is a result of groundwater recharge by leakage from irrigation canals, which is earlier defined as the largest and longest unintended anthropogenic recharge globally (MacAllister et al., 2022; Scanlon et al., 2023). Groundwater storage peaked in the 1970s. Between the 1970s and 2000, trends became spatially heterogeneous: while some areas continued to experience rising groundwater levels due to sustained canal leakage recharge, others began to show declines associated with increasing groundwater abstraction. Overall, groundwater level changes from 1900 to 2010 reflect the evolving interplay among canal construction, abstraction, and precipitation variability (MacAllister et al., 2022). However the magnitude and relative contributions of different recharge and abstraction components to the observed changes remain unclear. In particular, the roles of sector-specific abstractions (irrigation, domestic, and industrial use) and irrigation return flows in shaping groundwater dynamics are insufficiently constrained.

At the global level, Scanlon et al. (2023) have shown that groundwater recharge and abstractions not only affect groundwater table depth but also affects the interaction with surface water. De Graaf et al. (2019) showed how groundwater table changes may affect groundwater-surface water interactions that amongst others affects environmental river flows. Maheswaran et al. (2016), using a regional groundwater model, suggested that parts of the Ganges and Yamuna may have shifted from draining to infiltrating due to local abstractions. However, the evolution of these interactions since canal construction in the mid-19th century has been unknown. Local tributaries also play a key role (de Vries, 1995), yet their historical changes remain undocumented.

The surface water–groundwater (SW–GW) interactions are important to understand as it also highly impacts the surface water quality. Reduced baseflow limits pollutant dilution, while contaminated river water can infiltrate into aquifers (van Broekhoven et al., 2024), posing public health risks when groundwater is used as source for drinking water (Lewis, 2007).

Despite our understanding of long-term groundwater table trends, a deeper understanding of the historical and spatial evolution of groundwater balance components, including how water-use sectors and return flows developed over time, is crucial for improving predictions and designing effective management strategies to protect water resources, environmental flows, and

https://doi.org/10.5194/egusphere-2026-1584
Preprint. Discussion started: 31 March 2026

community well-being. A better understanding of historical system behaviour is beneficial to set realistic restoration objectives (Forstner et al., 2025).

Long-term monitoring data are only available for the northwestern IGB (Punjab and Haryana). How groundwater table depth and SW–GW interactions have responded to variations in recharge and abstraction in the more humid eastern region, e.g. state of Uttar Pradesh, remains unknown. We focus on the Upper Ganges-Yamuna interfluve, which contains the Hindon River, as the water system in this region is heavily modified by human activity (van Broekhoven et al., 2024).

This study aims to quantify the spatio-temporal evolution of groundwater recharge and abstraction components, and their effects on groundwater tables and GW–SW interactions in the Upper Ganges–Yamuna interfluve of the IGB. These processes will be simulated using a spatially explicit, physically based groundwater model (MODFLOW 6), covering two centuries from pre-canal conditions (< 1830) to recent times (2016). This will improve understanding on the contribution of different water use sectors to groundwater dynamics as a starting point for policies on sustainable groundwater management.

2 Study area and methods

2.1 The Upper Ganges-Yamuna interfluve

The Upper Ganges-Yamuna interfluve (Figure 1) is part of the Ganges basin. It is located in western Uttar Pradesh and southern Uttarakhand, India, situated north of Delhi. The Hindon River subbasin, located at the centre of the study area, is a rainfed tributary of the Yamuna that originates in the Shivalik Hills and is joined by its tributaries, Krishni and Kali Rivers (van Broekhoven et al., 2024). The region has a humid subtropical climate, with most rainfall occurring during the monsoon season (June–September), around 700–950 mm, while the non-monsoon period (October–May) receives only about 100–200 mm of rainfall (Mourad et al., 2024).

Hydrogeologically, the subbasin is part of the Indo-Gangetic alluvial aquifer system, comprising thick sequences (up to more than 200 m) of medium- to coarse-grained oxidized sands with high hydraulic conductivity (30–50 m/d) that can be largely considered as a single aquifer (Bonsor et al., 2017). Depths of groundwater table typically range from a few meters up to more than 30 meters, with deeper water tables occurring in coarse alluvial deposits along the basin's northern margin (Alam & Umar, 2013; Bonsor et al., 2017; Umar et al., 2008; Van Dijk et al., 2020). A regional north-to-south gradient of approximately 0.55 m/km characterizes the flat topography (van Broekhoven et al., 2024).

Groundwater extraction has increased substantially since the mid-20th century due to agricultural intensification and urban expansion. While early irrigation primarily relied on canal networks, such as the Upper Ganga Canal built in 1854 (Drew, 2014) and the Eastern Yamuna Canal constructed in 1830 (Irrigation and Water Resources Department, n.d.), the post-Green Revolution period marked a shift toward intensive groundwater use (Pingali, 2012). This transition was driven by technological advancements, including the adoption of hand pumps, diesel pumps and electric pumps, as well as policy incentives promoting groundwater use, such as the provision of free electricity for irrigation (Panda et al., 2021). As a result, groundwater tables dropped (Jadav & Yadav, 2025; Mendoza et al., 2026). This has contributed to the reduced flow of the Hindon River outside

https://doi.org/10.5194/egusphere-2026-1584
Preprint. Discussion started: 31 March 2026

the monsoon season, particularly in its headwaters, which are now ephemeral (van Broekhoven et al., 2024). As groundwater tables continue to fall, sections of the river may have shifted from draining to infiltrating from the river into the surrounding aquifer (van Broekhoven et al., 2024).

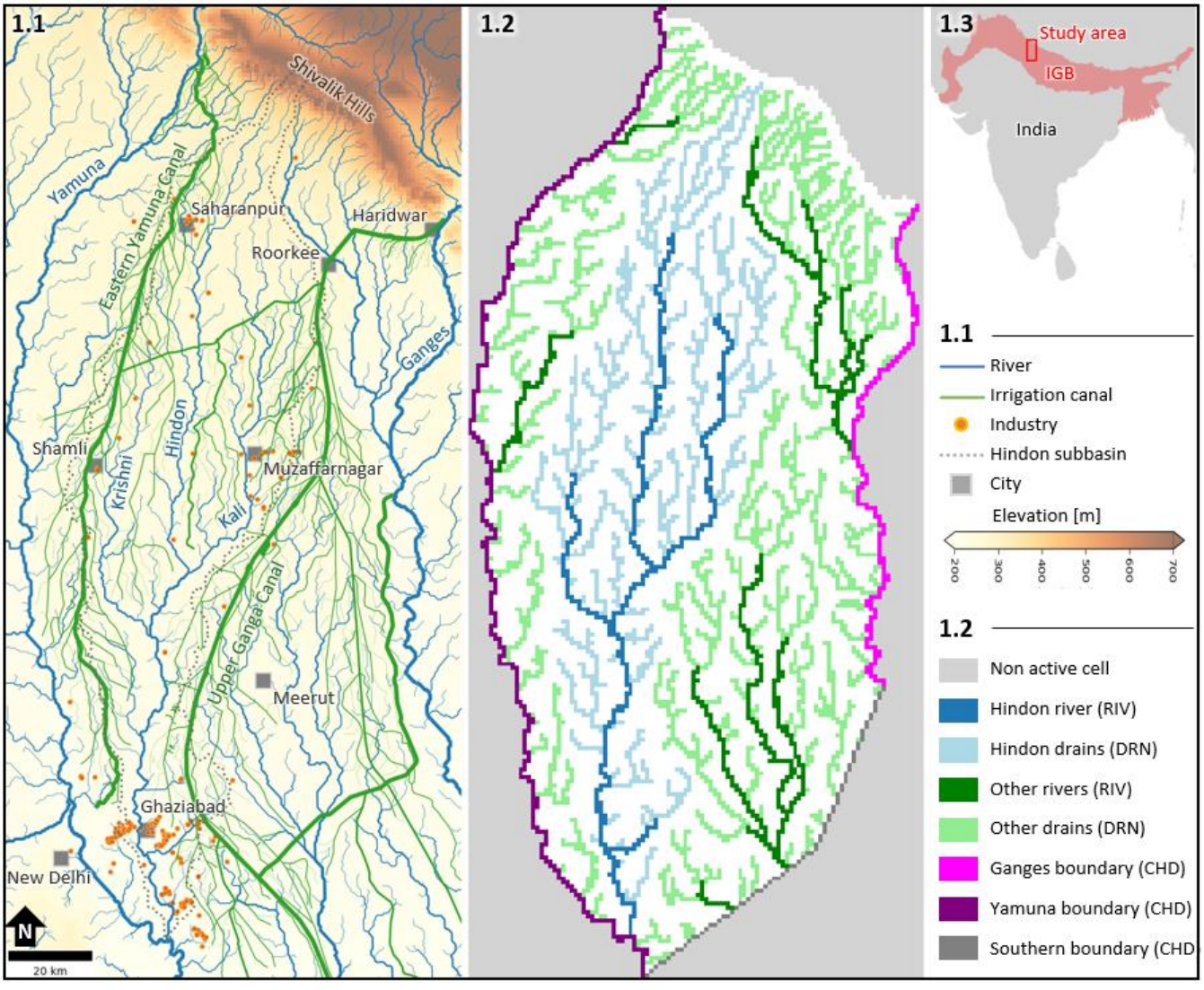

Figure 1: 1.1) Study area with rivers, irrigation canals and surface elevation (HydroSHEDS, Lehner et al., 2008). 1.2) MODFLOW model schematisation of rivers and boundaries (MODFLOW package names shown in brackets). 1.3) Location of study area within the Indo-Gangetic Basin (IGB). IGB outline is adapted from Bonsor et al. (2017).

2.2 MODFLOW 6 – model schematisation

The complex interplay between recharge, abstractions, groundwater table depth, and groundwater–surface water interaction was modelled using MODFLOW 6 (Langevin et al., 2017). This spatially explicit, process-based model incorporates the spatial

https://doi.org/10.5194/egusphere-2026-1584
Preprint. Discussion started: 31 March 2026

and temporal distribution of recharge and abstraction components. These processes are the primary drivers of groundwater balance change. However, quantifying these components and subsurface properties requires assumptions, introducing uncertainties. To address this, multiple schematizations of subsurface properties and recharge and abstraction inputs were used to generate a wide range of scenarios. Unrealistic scenarios were filtered out, resulting in narrower parameter ranges.

This study used a transient MODFLOW 6 model with a regular grid consisting of a single layer, 231 rows, and 108 columns, with 1000 m × 1000 m cells. The model was set up and analysed using the Flopy Python package (Bakker et al., 2016). A high spatial resolution was selected due to the observed variability in recent groundwater trends (Joshi et al., 2021; Van Dijk et al., 2020) and findings by Van Broekhoven et al. (2024), which indicate that recharge components such as canal leakage have highly localized influences (< 1 km) based on groundwater quality signatures. The simulation period spans over two centuries (1800–2016) in yearly time steps, covering pre-canal development to the present.

The aquifer was represented as a single hydrogeological unit using one model layer, due to discontinuous and local clay layers (Bonsor et al., 2017). This is consistent with the schematization of Maheswaran et al. (2016), who applied a uniform aquifer thickness of 200 m. The model top elevation was derived by resampling the mean elevation from the HydroSHEDS Digital Elevation Model (DEM) (Lehner et al., 2008).

Model boundaries were defined to reflect natural hydrogeological system limits where possible. The eastern and western boundaries are defined by the Ganges and Yamuna rivers and were simulated as Constant Head Boundaries, assuming groundwater head equal river levels due to their size and strong hydraulic connection. Because a yearly time step was applied, seasonal variability was not included. Furthermore, the use of Constant Head boundaries implies that interannual variability in average river stages is assumed to be limited. The northern boundary is defined by the Shivalik Hills and treated as a no-flow boundary. Along the southern boundary, where no clear natural border exists, a constant head boundary was set sufficiently far (>10 km) from the Hindon subbasin to minimize edge effects.

The Hindon River and its main tributaries are simulated by the RIV package, allowing for both infiltration and exfiltration, as the river is effluent-fed and flows year-round, with indications of ongoing infiltration (van Broekhoven et al., 2024). Smaller streams and drains, which typically dry up outside the monsoon season, were simulated using the DRN package, permitting only discharge. Water levels for rivers, drains, and constant head boundaries (including the Ganges and Yamuna rivers) were set equal to the resampled minimum elevation value from the HydroSHEDS DEM (Lehner et al., 2008).

The model focuses on the spatial and temporal variation of recharge and abstractions. Recharge components include rainfall, canal water leakage, irrigation return flow, and municipal return flow. Sectoral water withdrawals include irrigation, municipal, and industrial uses. These model forcings (recharge and abstraction) generate outputs such as groundwater table depths and fluxes across boundaries, rivers, and drains. Figure 2 illustrates the groundwater balance components, with black arrows representing model inputs and blue arrows indicating model outputs.

Spatio-temporal information was required for each recharge and abstraction component over the simulation period. As such datasets are not readily available, multiple data sources were integrated and informed assumptions were applied to derive

https://doi.org/10.5194/egusphere-2026-1584
Preprint. Discussion started: 31 March 2026

spatially and temporally consistent estimates for each component. In general, available spatially explicit data were used for the current situation, while historical data were collected to establish trendlines to hindcast past conditions. The aim was to capture overall temporal trends in a spatially distributed manner rather than precise estimates for each cell and time step. The construction of spatio-temporal datasets for all recharge and abstraction components per model cell and time step is described in Appendix A.

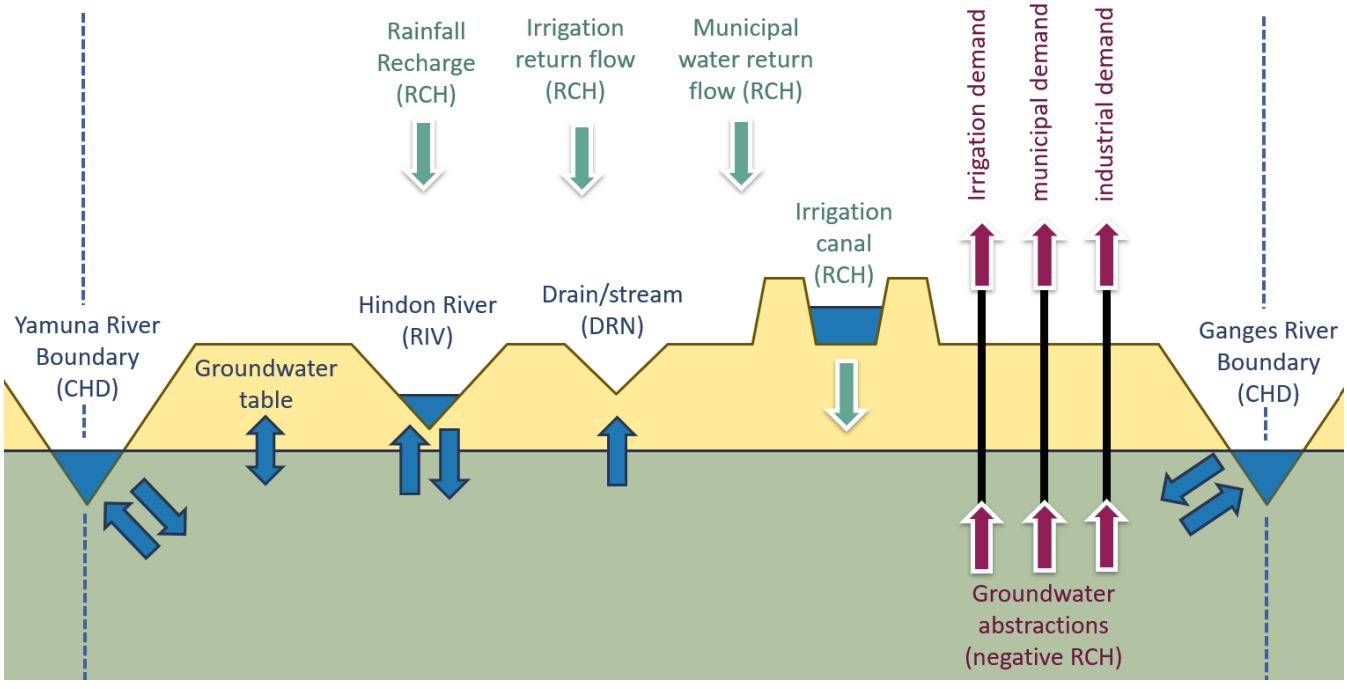

Figure 2. Conceptual representation of groundwater balance components in the model domain. Green arrows indicate model input fluxes (forcing) representing recharge sources, while red arrows indicate model input fluxes (forcing) representing groundwater abstractions (simulated as negative recharge). Blue arrows represent fluxes simulated by the model (i.e., model outputs), including groundwater–surface water exchanges and boundary flows (MODFLOW package names shown in brackets).

2.3 Monte Carlo analysis and validation

We used the Monte Carlo method to account for uncertainty in input data (e.g. Ballio & Guadagnini, 2004; Bekesi & McConchie, 1999; Kahe et al., 2021). Table 1 shows the prior parameter ranges for hydraulic conductivity, aquifer thickness, and specific yield derived from the literature. To maximize scenario variability, we assumed uniform probability distributions for these parameter ranges. River and drain conductivity had log-uniform probability distribution (Table 1)

For computational efficiency, we combined all recharge and abstraction components into a net recharge variable, calculated as the sum of all recharge minus abstractions components. Since the model uses a single layer, abstractions could be treated as negative recharge. We applied uniform uncertainty factors between 0.25 and 4 to each component, except for rainfall recharge where we considered between 0.5 and 2 more realistic (see Table 2). This preserves temporal trends and spatial variations per

https://doi.org/10.5194/egusphere-2026-1584
Preprint. Discussion started: 31 March 2026

component, but for the cumulative net recharge, this yields temporally and spatially varied values across scenario runs. Log-uniform probability distributions were used for each multiplication factor to get a uniform distribution of factors bigger and smaller than the initial estimate.

Table 1: Bandwidth of prior aquifer properties parameters.

Parameter	Min	Max	Distribution	References
Conductivity K [m/day]	5	100	Uniform	10- 70 m/day (Bonsor et al., 2017). 19.5 - 40.1 m/day (Alam and Umar, 2013) 11.0 – 26.6 m/day (Maheswaran et al., 2016)
Aquifer thickness [m]	50	250	Uniform	Up to more than 200 m (Bonsor et al., 2017) 38.4 – 118.2 m (Alam and Umar, 2013) 200 m (Maheswaran et al., 2016)
River conductivity [m^2/day]*	0.001 × A	10 × A	Log-uniform	256 to 410 m^2/day (Alam and Umar, 2013) 30 - 150 m^2/day (Maheswaran et al., 2016)
Drain conductivity [m^2/day]*	0.001 × A	10 × A	Log-uniform	
Specific yield [-]	0.05	0.35	Uniform	0.10 - 0.25 (Bonsor et al., 2017) 0.10 - 0.20 (Alam and Umar, 2013). 0.15 (Maheswaran et al., 2016)

***The river and drain conductivity is calculated by the surface water area per cell (A) multiplied by the vertical leakage coefficient (which is the riverbed conductivity divided by riverbed thickness and has unit day^{-1}). The surface water area per cell (A) varies for each model cell from 151 to 10,960 m2 for river cells and from 2.6 to 22,425 m2 for drain cells.**

Table 2: Multiplication factors for recharge and abstraction components (prior parameter ranges), log-uniform distribution.

Recharge and abstraction components	Min	Initial	Max	Distribution
Irrigation groundwater demand	0.25	1.00	4.00	Log-uniform
Municipal groundwater demand	0.25	1.00	4.00	Log-uniform
Industrial groundwater demand	0.25	1.00	4.00	Log-uniform
Rainfall recharge	0.50	1.00	2.00	Log-uniform
Canal leakage recharge	0.25	1.00	4.00	Log-uniform
Irrigation return flow recharge	0.25	1.00	4.00	Log-uniform
Municipal return flow recharge	0.25	1.00	4.00	Log-uniform

The model executed 1500 simulation runs, each with randomly sampled aquifer properties, and net recharge derived from the separate recharge and abstraction components with random multiplication factors. To stabilize initial conditions, each run had a 100-year warm-up period.

https://doi.org/10.5194/egusphere-2026-1584
Preprint. Discussion started: 31 March 2026

All model runs were evaluated against observational data and subjected to constraints to ensure realistic outcomes. Regarding observational data, groundwater level data from 94 observation wells (containing data between 1990–2018) with at least 10 years of monitoring data were used for evaluation. Data availability varied in space and time, some wells were recorded 4 times a year, while others were measured incidentally. We used the Mean Absolute Error (MAE) as a measure of goodness in fit and the Mean Error as a measure of bias. Both objective functions are robust against outliers as they do not use squared values and are easily interpretable as both measures have the same units as the observations. We accepted all model runs with Mean Absolute Error (MAE) ≤ 7.5 m and Mean Error (bias) between –5 m and +5 m.

To ensure physically plausible system behaviour beyond the observation period, model runs were screened using four realism criteria: (i) when simulated groundwater tables exceeded ground level in more than 2.5% of active cells, since extensive wetlands or persistent surface waterlogging are not reported for the study area; (ii) when more than 5% of active cells showed groundwater depths greater than 50 m below ground level, since across most of the study area groundwater is widely used and easily accessible and thus shallower; (iii) the simulated yearly average baseflow of the Hindon River for the period 1997–1999 must not exceed 65 m^3/s. This threshold represents the mean observed discharge (65 m^3/s) measured at Mohannagar between April 1997 and March 1999 (Jain and Sharma, 2006) and limits unrealistically high groundwater contributions to river discharge (> 100 %); (iv) under natural (pre-canal: < 1800) conditions, the simulated yearly average baseflow in the Hindon River subbasin was required to remain positive (> 0 m^3/s), reflecting expected groundwater exfiltration to the river in the absence of major anthropogenic alterations. Only runs that performed adequately against observations and realism checks were retained.

From the 1,500 simulations, 198 runs (13%) were unsuccessful due to numerical instability. Among the remaining 1,302 runs, 196 met all performance and realism criteria and were classified as valid. Figure 3 presents histograms of the parameter distributions for the prior ensemble and the subset of valid model runs. Comparison of the valid runs with the full ensemble shows that the valid models generally have higher aquifer conductivity and thickness and also higher river bed and drain bed conductivity. Additionally model validity was further influenced by recharge and abstraction factors. Rainfall recharge factors greater than 1 resulted in fewer valid runs, as did irrigation demand factors exceeding 1.5.

https://doi.org/10.5194/egusphere-2026-1584
Preprint. Discussion started: 31 March 2026

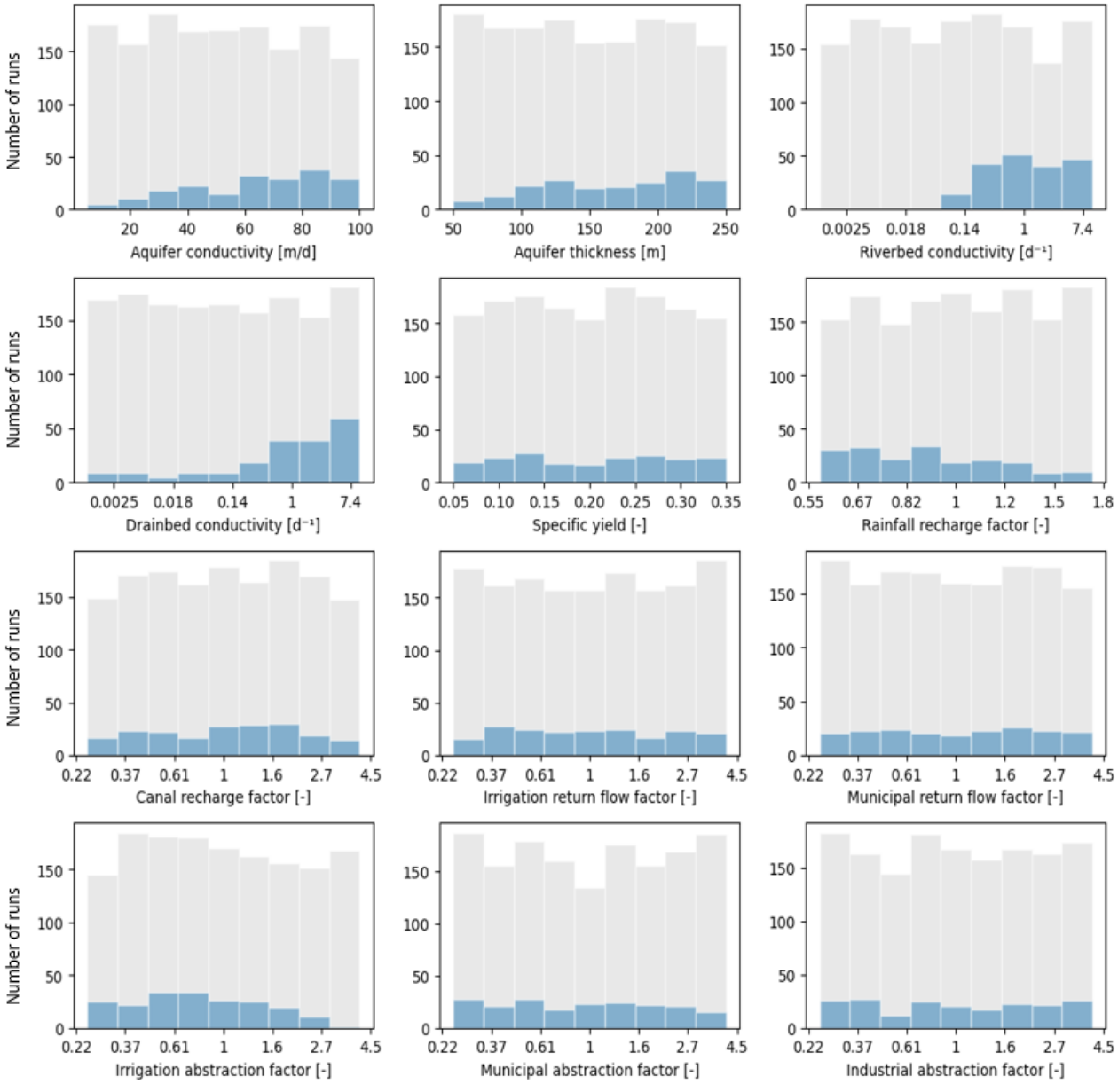

Figure 3. Parameter distribution priors (grey) and the posterior valid runs (blue).

3 Results

3.1 Dynamics in recharge and abstraction components

Figure 4 illustrates the initial estimates of recharge and abstraction components since 1800, revealing distinct shifts in groundwater usage. Only after 1900 there was information on annual precipitation variability by CRU TS. Up to 1830, the

https://doi.org/10.5194/egusphere-2026-1584
Preprint. Discussion started: 31 March 2026

system was dominated by natural rainfall recharge, which formed the primary input to the groundwater system. With the construction of the irrigation canal network since 1830, recharge volumes increased, augmenting the overall groundwater balance. However, from the 1970s onward, a pronounced rise in groundwater abstractions marked a transition toward increasing anthropogenic pressure directly on groundwater. This trend intensified between 1980 until 2010. The groundwater abstraction rates increase seem to flatten in the last decade. Currently, the primary recharge components are rainfall (approx. 50-80%) and irrigation return flow (approx. 10-25%), followed by canal leakage (approx. 10%), with municipal water return flow contributing to a minor extent (approx. 2.5%). Conversely, irrigation remains the dominant component of groundwater abstraction (approx. 80-85%), with municipal (approx. 10-20%) and industrial (< 1%) uses accounting for smaller, though locally sometimes significant, proportions.

The black line in Figure 4 represents the net recharge, which is up to 1940 equal to the rainfall recharge, and is calculated as the sum of all recharge components minus all abstractions. A negative net recharge indicates that, on an annual basis, more groundwater is abstracted than recharged. Figure 5 illustrates the bandwidth of net recharge when input uncertainties are considered and valid model runs are selected. Net recharge first increased by canal recharge, but within the uncertainty bands in 1970 and on average around 2000, the system has been characterized by also negative net recharge. Uncertainty ranges are higher after 2000, due to the multiple components that become relevant for the net recharge.

Figure 6 shows the spatial variation of recharge (+) and abstraction (-) components averaged over several time periods. Rainfall recharge exhibits the highest rates along the Shivalik Hills (northeast) and gradually decreases towards the southwest. Also a decrease in time is observed, although the declining gradient from northeast to southwest stays constant. Canal leakage is concentrated along the main canal network and is lower along secondary branches. Over time, newly developed canal areas become visible, although their extent remains relatively small compared to the main irrigation network. Irrigation return flow (recharge) and irrigation demand (abstraction) are distributed fairly evenly across the region, except in the north along the Shivalik Hills and in the south around urban settlements such as Ghaziabad, where there is limited irrigation. Municipal return flow and municipal demand are highly localized around major towns, with clear hotspots at Ghaziabad, Meerut, Muzaffarnagar and Saharanpur. Industrial demand is also associated with municipal areas but is more sparsely distributed. Net recharge remains predominantly positive until 2000. During the period 1970–2000, negative net recharge (i.e., abstractions exceeding recharge) is mainly limited to areas around Ghaziabad. After 2000, large parts of the region exhibit negative net recharge, with a broad north–south division emerging around the latitude of Muzaffarnagar, separating predominantly positive conditions in the north from negative conditions in the south.

https://doi.org/10.5194/egusphere-2026-1584
Preprint. Discussion started: 31 March 2026

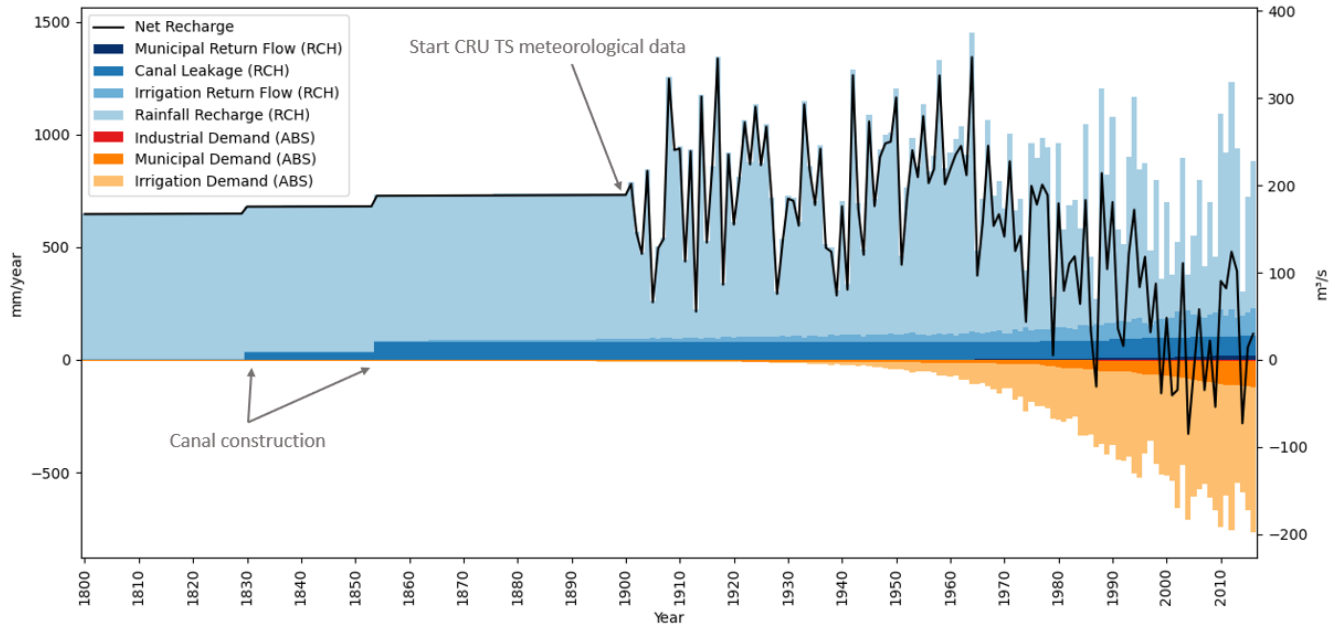

Figure 4: Initial estimates of changes in recharge (+) and abstractions (-) components (black line = net recharge, which is sum of all recharge minus all abstractions components).

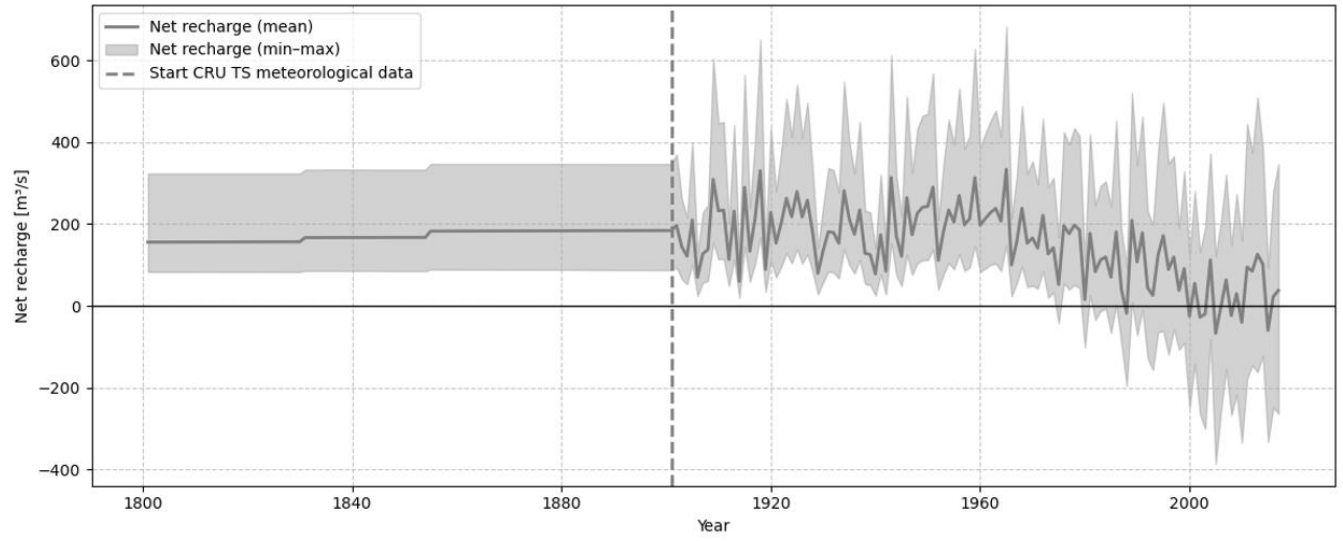

Figure 5. Net recharge input of the valid model runs (min, mean, max). Net recharge is calculated as the sum of all recharge (+) minus all abstractions (-) components

https://doi.org/10.5194/egusphere-2026-1584
Preprint. Discussion started: 31 March 2026

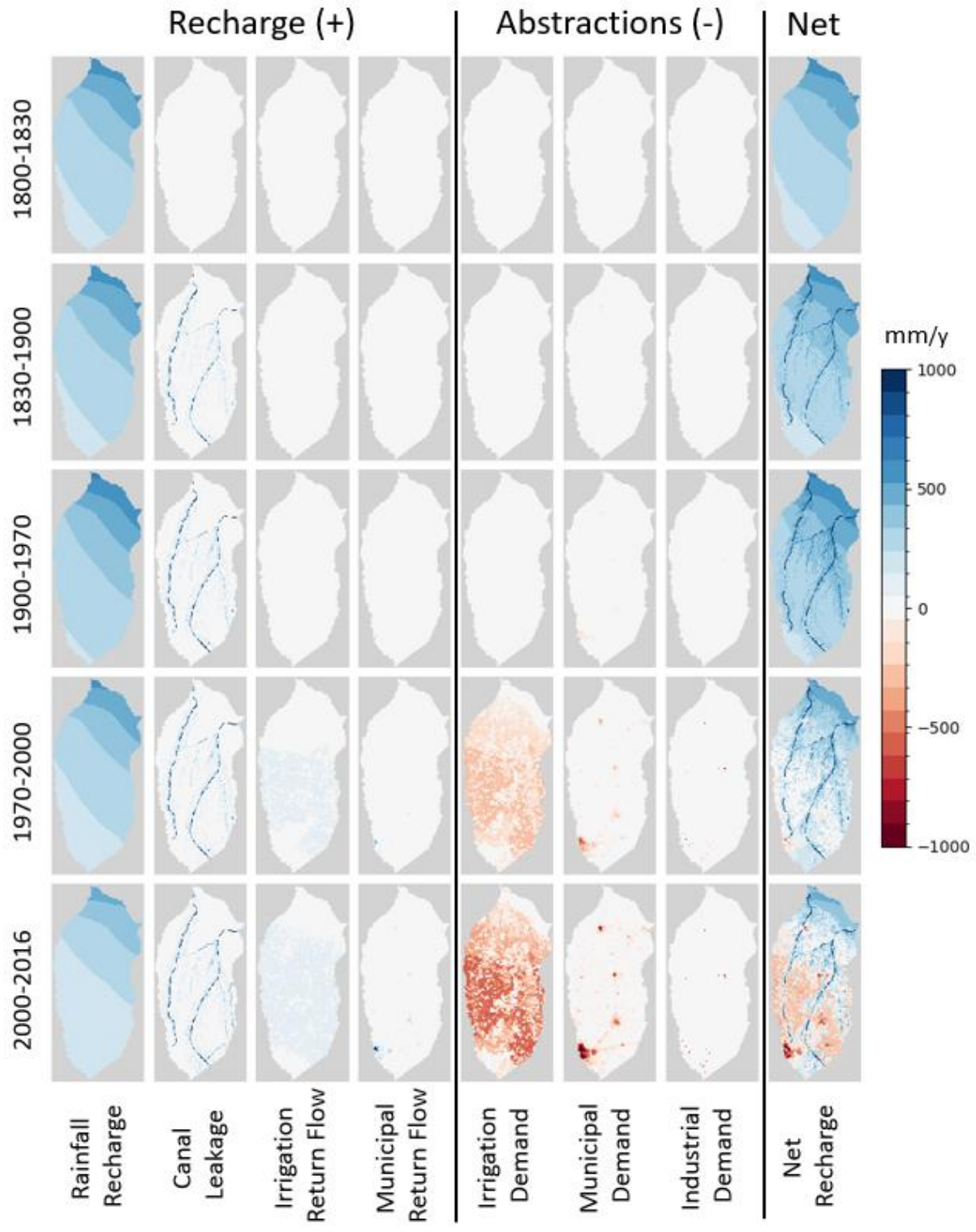

Figure 6. Spatial variation of initial estimates of recharge (+) and abstractions (-) components during time periods.

https://doi.org/10.5194/egusphere-2026-1584
Preprint. Discussion started: 31 March 2026

3.2 Effects on groundwater table

Figure 7 depicts groundwater table trends based on spatial median values. We used the mean of spatial medians per time step and model run to avoid bias toward deeper tables caused by the deep groundwater table in the Shivalik Hills. Groundwater table trends are closely aligned with those of net recharge. Following the construction of canals since 1830, median groundwater tables rose by approximately 0.5 to 1.0 meter over the entire study area. From 1900 to 1970, groundwater tables increased slightly but generally remained stable. The annual variability is also depicted since 1900. However, since the 1970s, a marked and accelerating decline in groundwater tables has been observed. By 2016, the median groundwater table depth had increased to an average of 10 meters, compared to approximately 7.5-8.0 meters in the pre-1830 "natural situation."

Figure 8 shows spatial maps of depth of groundwater tables for the natural pre-1830 and current situations, together with maps showing the differences for the intermediate periods. Overall, groundwater table is deeper in the Shivalik Hills, in the area between the lower reaches of the Yamuna River and the Hindon River, and along the left bank of the Ganges River. These areas coincide with higher ground elevations. The regional groundwater gradient generally follows a north–south direction. The first difference map indicates increasing groundwater tables, mainly around the irrigation canals. The second period (1830–1900 versus 1900–1970) reflects relatively high rainfall recharge in the Shivalik Hills during 1900–1970. Since the 1970s, groundwater table declines are visible across most of the study area. Near the rivers, declines are negligible, whereas areas farther from the rivers show the most pronounced groundwater table declines. After 2000, groundwater tables declined further.

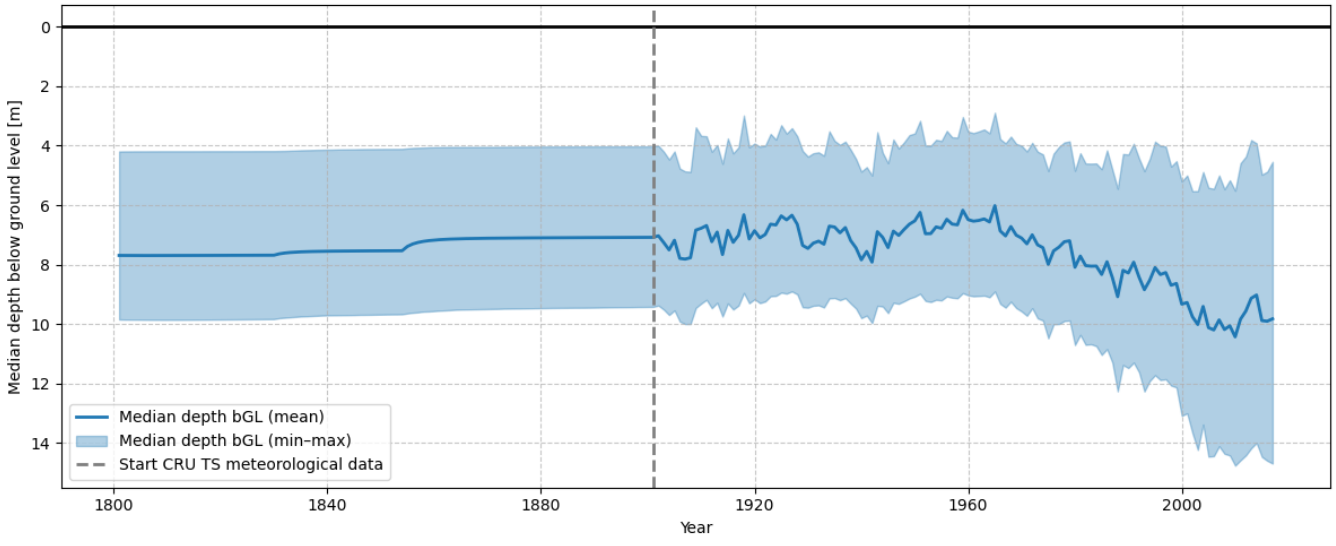

Figure 7: Median depth of groundwater table per time step, showing the ensemble minimum, mean and maximum across valid model runs.

https://doi.org/10.5194/egusphere-2026-1584
Preprint. Discussion started: 31 March 2026

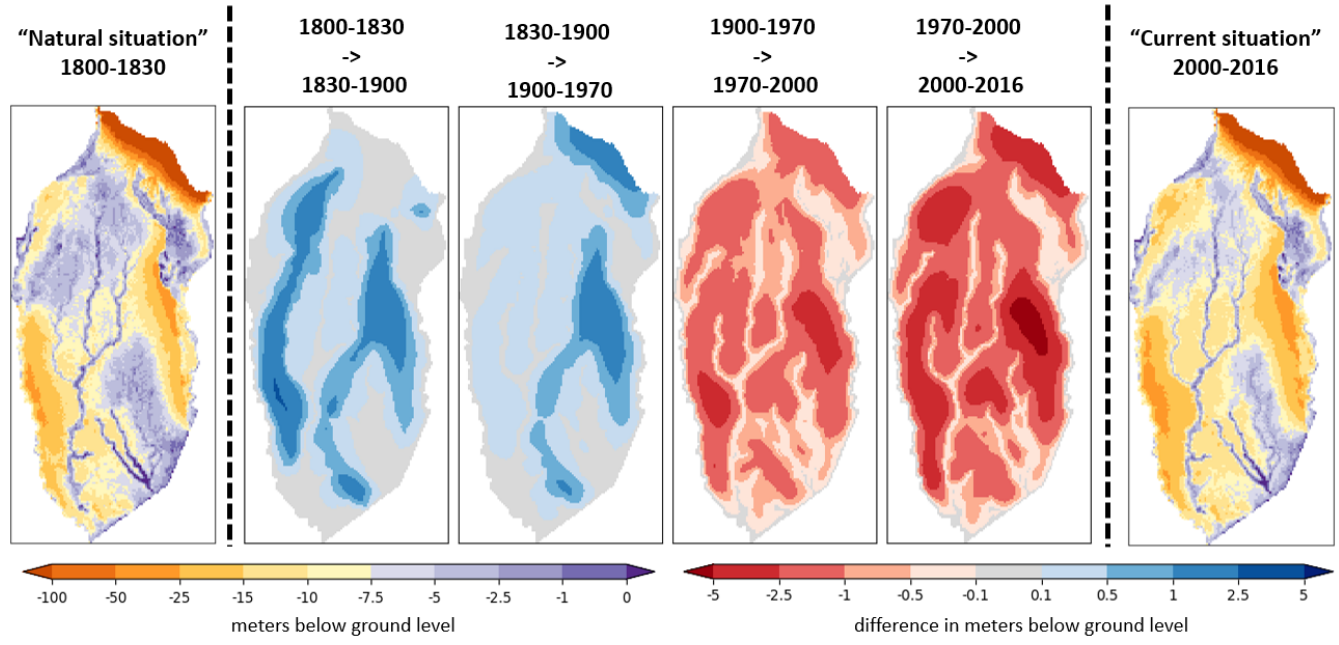

Figure 8: Depth of groundwater tables below ground level for natural and current situation (most left and right) and difference between time periods (middle 4).

3.3 Effects on groundwater – surface water interactions

Figure 9 shows the temporal variation in groundwater exfiltration fluxes to river surface water on the Upper Ganges–Yamuna interfluve (Hindon River and other local rivers), and to the adjacent reaches of the Ganges River and Yamuna River. Exfiltration refers to groundwater drainage and discharge from the aquifer to surface water bodies. A positive exfiltration flux indicates groundwater flow to the river, whereas a negative flux indicates infiltration of river water into the aquifer. During the pre-groundwater-exploration period (before the 1970s), Hindon River and other local rivers, captured the majority of groundwater seepage, while only a smaller fraction discharged directly into the main channels of the Ganges and Yamuna. Groundwater outflow along the southern gradient is neglectable and thus excluded from the figure.

The trends in groundwater exfiltration fluxes closely follow those of net recharge and groundwater table depth. The construction of irrigation canals introduced additional recharge, which in turn increased groundwater exfiltration. Since the 1970s, however, groundwater exploration has led to a decline in exfiltration. This reduction is particularly pronounced in the Hindon River network, where most model runs indicate a shift from exfiltration to infiltration since around 2000. This implies the river on average now infiltrates more water year-round than it receives from groundwater. While some model runs suggest this switch began as early as the 1970s, others do not show a switch at all. Groundwater exfiltration to the adjacent reaches of the Ganges and Yamuna rivers has also declined, but nearly all model runs still indicate net exfiltration.

Figure 10 presents the spatial variation of surface water–groundwater interactions averaged over different time periods. The results predominantly show exfiltrating reaches for the 'natural situation', interspersed with several infiltrating reaches.

https://doi.org/10.5194/egusphere-2026-1584
Preprint. Discussion started: 31 March 2026

Although groundwater table declines are spatially most pronounced near the canal network, changes in surface water–groundwater exchange are more widespread, with many river reaches showing increased infiltration or reduced exfiltration, after the construction of the irrigation canals. Similar patterns are observed in subsequent periods, with conditions largely reversing after the 1970s. Since around 2000, most of the Hindon River has shifted to an infiltrating state, whereas the sections near the Shivalik Hills foothills continue to be mainly exfiltrating.

https://doi.org/10.5194/egusphere-2026-1584
Preprint. Discussion started: 31 March 2026

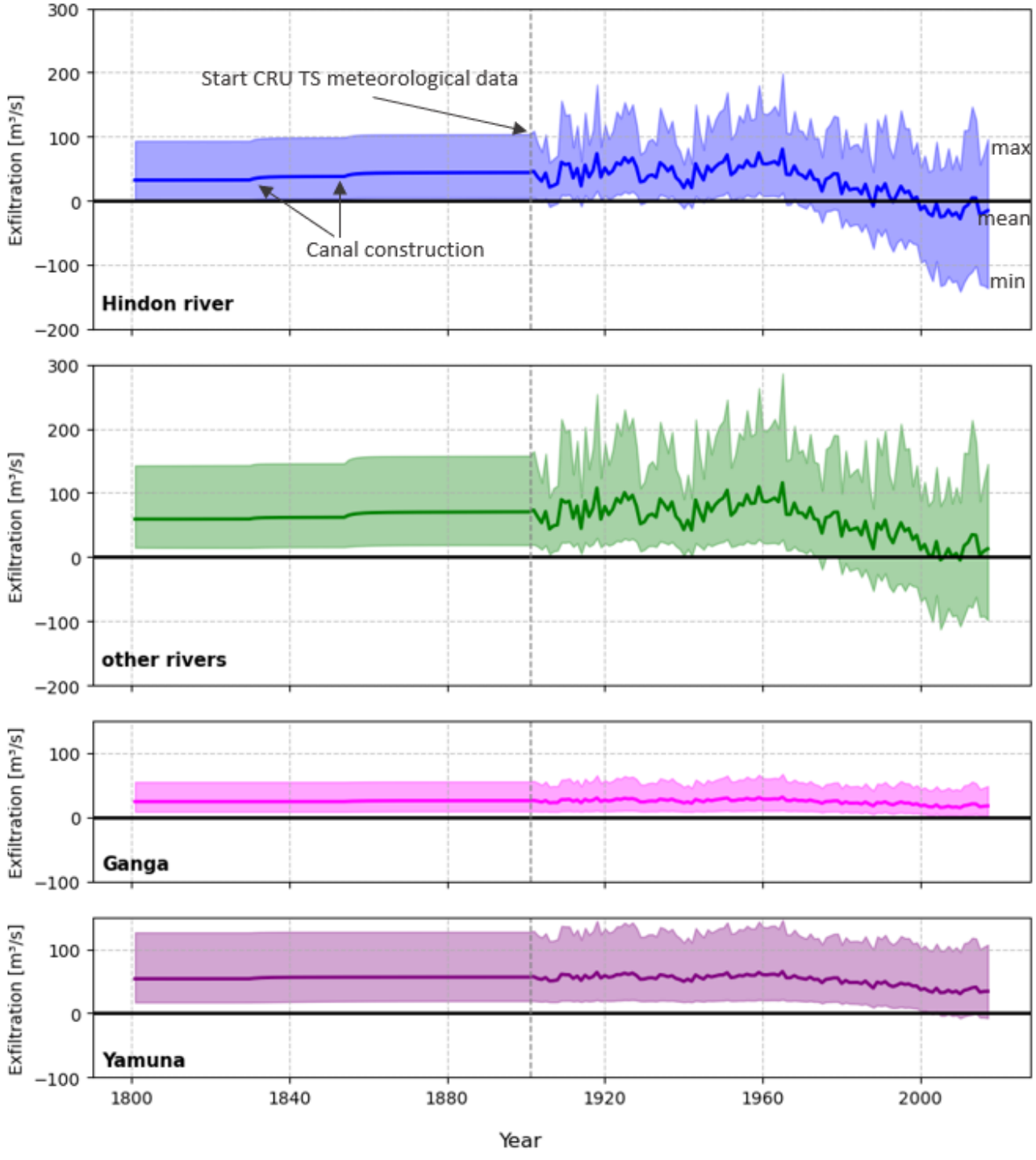

Figure 9: Exfiltration fluxes of groundwater to river surface water of the valid model runs (min, mean, max) of the Hindon River, other local rivers on the interfluve and the adjacent reaches of the Ganges and Yamuna rivers. A positive exfiltration flux indicates groundwater flow to the river, whereas a negative flux indicates infiltration of river water into the aquifer.

https://doi.org/10.5194/egusphere-2026-1584
Preprint. Discussion started: 31 March 2026

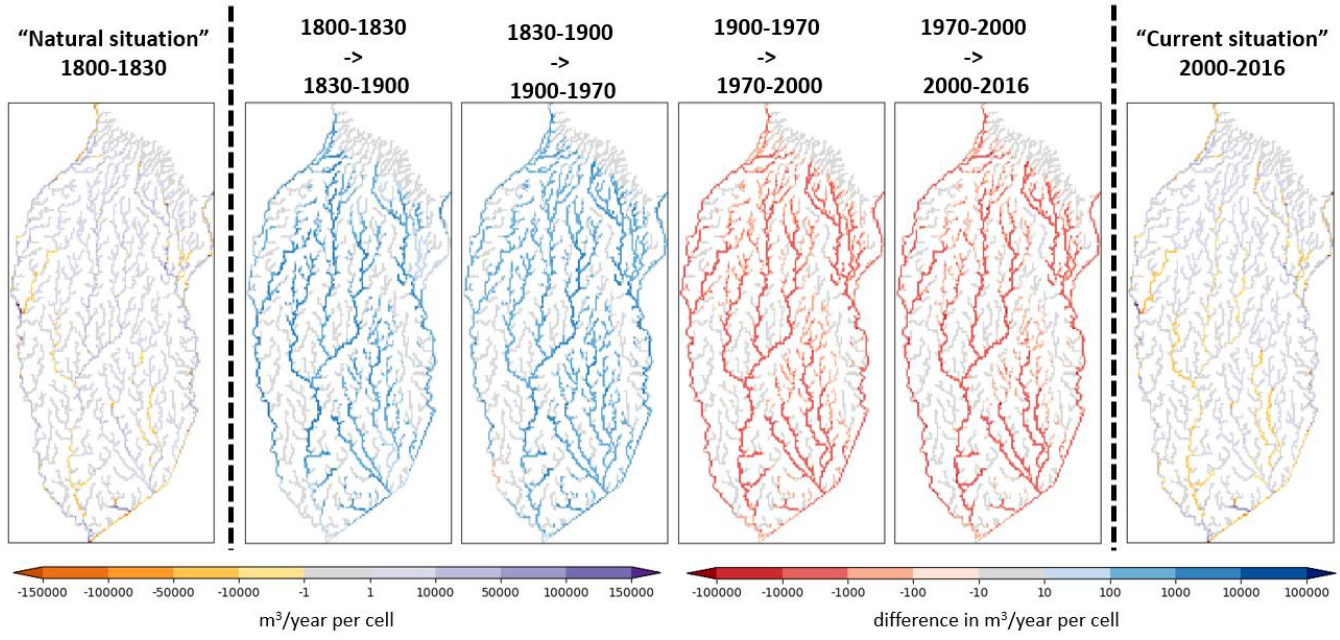

Figure 10: Spatial variation of groundwater–surface water interaction, expressed as exfiltration (+) and infiltration (−), for the natural and current situations (left and right panels, respectively), and the differences between time periods (four middle panels).

4 Discussion

4.1 Groundwater balance evolution over the past two centuries in the Upper Ganges-Yamuna interfluve

Changes in groundwater recharge or abstraction influence groundwater levels with a temporal delay, as the system adjusts to shifts in storage. This, in turn, alters groundwater-surface water (GW-SW) interactions until a new equilibrium is reached (de Graaf et al., 2019; Bierkens & Wada, 2019; Scanlon et al. (2023). In practice, increased or decreased recharge leads over time to a new stable state with correspondingly higher or lower groundwater tables and exfiltration rate to rivers.

Figure 11 schematizes how the groundwater balance in the Upper Ganges-Yamuna interfluve has evolved over the past two centuries. We identify five distinct time slices characterizing this evolution:

1) Natural situation (1800 – 1830): A near-natural state where recharge is dominated by rainfall, the system is in balance, and groundwater tables are stable. Groundwater exfiltration to surface water more or less equals rainfall recharge.
2) Canal development (1830-1900): Canals enhance recharge, raising groundwater tables and increasing exfiltration. Our groundwater model illustrates this dynamic response following canal construction in 1830 (Eastern Yamuna Canal) and 1854 (Upper Ganga Canal). The system adjusts to the increased recharge, reaching a new equilibrium with elevated but stable groundwater tables and exfiltration rates.

https://doi.org/10.5194/egusphere-2026-1584
Preprint. Discussion started: 31 March 2026

3) Stable period (1900-1970): Long-term recharge is in equilibrium with long-term groundwater tables and exfiltration. Annual meteorological variability causes temporary fluctuations, with lower groundwater tables and exfiltration during dry periods and reversed during wet periods.
4) Groundwater development since Green Revolution (1970-2000): Increased irrigation demand is met by groundwater abstraction, reducing net recharge (recharge minus abstractions). This decline in recharge lowers groundwater tables and exfiltration rates.
5) Current period with intensive groundwater use (2000-2016): Groundwater abstractions exceed recharge, resulting in negative net recharge, rapidly declining groundwater tables, and a shift from draining to infiltrating local rivers.

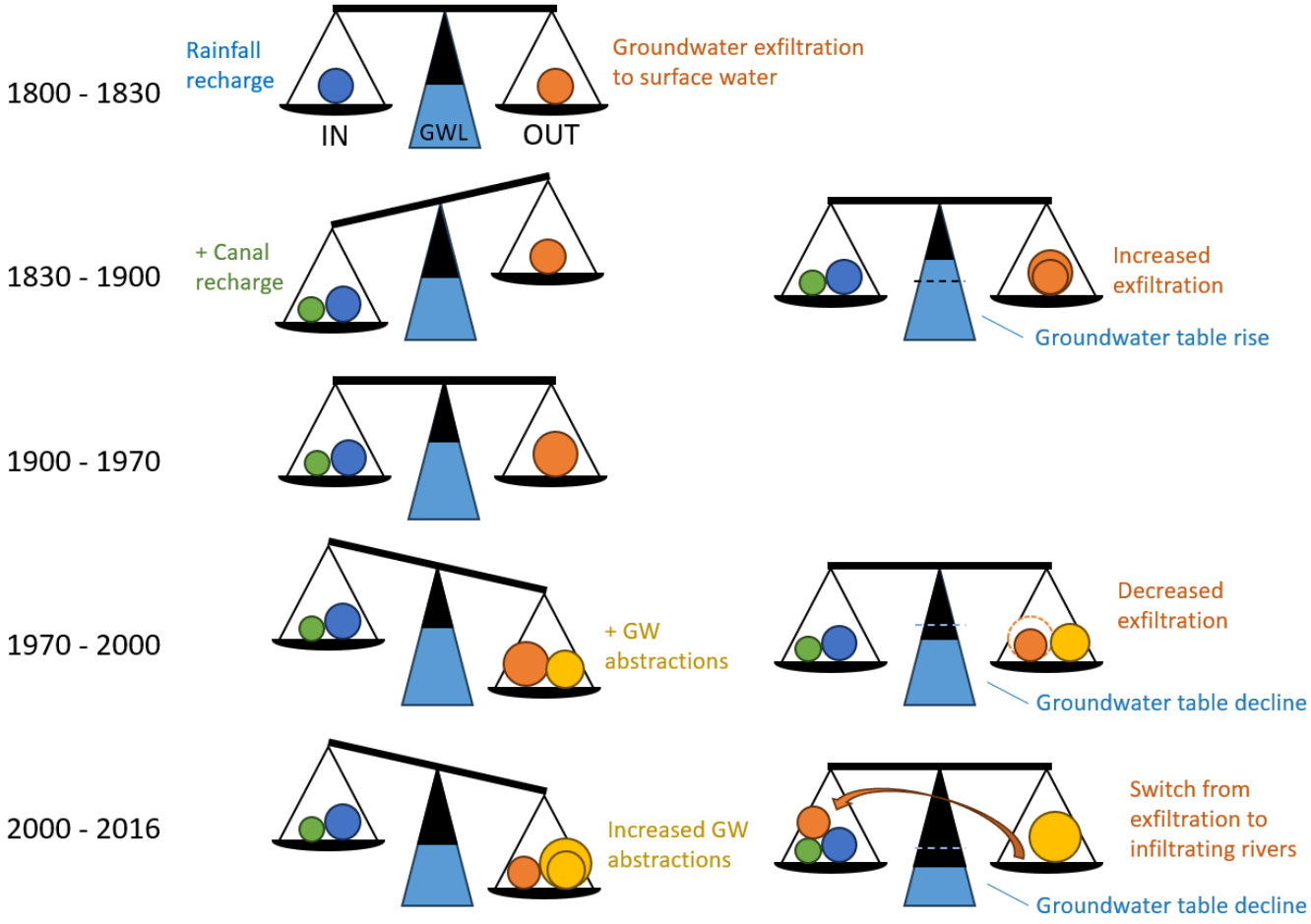

Figure 11. Changes in groundwater (GW) balance in the Upper Ganges–Yamuna interfluve from 1800 to present, based on the balance framework of Scanlon et al. (2023). The left panel shows system instability caused by changes in GW recharge or abstractions, while the right panel shows the system after adjustment to a new equilibrium, with altered groundwater tables and groundwater–surface water interactions.

https://doi.org/10.5194/egusphere-2026-1584
Preprint. Discussion started: 31 March 2026

The observed groundwater level rise from canal recharge aligns with MacAllister et al. (2022), though our study area shows smaller increases of 0.5–1 m on average (max 5 m) compared to their findings of several meters and up to 20 m in some locations. This discrepancy may stem from our area's wetter climate (located further east) or stronger surface water interaction, which limits storage changes. Additionally, a major difference is that the groundwater tables at our study area are currently below natural conditions (< 1830), whereas MacAllister et al. (2022) found current groundwater levels exceed those of a century ago. Panda et al. (2021) reported a groundwater storage decline equivalent to approximately 1 m when averaged uniformly across the study area between 1985 and 2013. Our findings indicate a median groundwater table decline of approximately 2 m over the same period, which can be considered comparable given the associated uncertainties.

Our results also reveal that local tributaries (e.g. Hindon River) to the Ganges and Yamuna have shifted from draining to infiltrating, while the main river channels of the Ganges and Yamuna still drain. This contradicts Maheswaran et al. (2016), who classified the Ganges and Yamuna currently as infiltrating rivers in this region. The different responses between local tributaries and the main river reaches may relate to the position of the local tributaries on the elevated interfluve, where groundwater table drops are most prominent, while the lower-lying main rivers form the regional drainage basis attracting groundwater flow from the surrounding areas (e.g. de Vries, 1995). This elevation-driven difference in hydrological setting also explains why the Hindon River and other interfluve rivers show the highest uncertainties: their higher elevation makes them more sensitive to groundwater table fluctuations (de Vries, 1995).

4.2 Model uncertainties and limitations

The model assumes spatial distribution of recharge and abstraction components remained constant over time, except for municipal demand/return flow, and canal leakage, which is a reasonable assumption given the usually stable land use patterns. Direct groundwater evaporation and root uptake from saturated groundwater are not represented, implying uptake occurs only from soil moisture. While appropriate under present-day low groundwater conditions, this assumption is more uncertain for historical periods when groundwater tables were likely higher. Under such conditions, neglecting evaporation and root uptake may lead to overestimation of simulated high groundwater tables.

Model sensitivity to river and drain levels is amplified by the flat topography of the study area. While HydroSHEDS data provides a baseline for riverbed elevations and water levels, its accuracy limitations could be addressed by incorporating local measurements in further research.

Temporal variations in annual river stages and dynamic coupling with surface water systems were not included in the model. While likely minor for the Hindon River, where wastewater dominates discharge, these omissions may be more relevant for the Ganges and Yamuna rivers, whose seasonal stages have been influenced by dams and irrigation infrastructure (Swarnkar et al., 2021).

The aquifer is represented as uniform and homogeneous as also in Maheswaran et al. (2016), despite reported heterogeneity (e.g. Bonsor et al., 2017). This simplification ensures that model responses primarily reflect spatio-temporal variations in net recharge and surface water boundary conditions rather than poorly constrained hydrogeological complexity. Given that aquifer

https://doi.org/10.5194/egusphere-2026-1584
Preprint. Discussion started: 31 March 2026

properties have not substantially changed over the past two centuries, this assumption is unlikely to affect the simulated temporal dynamics. However, due to homogeneous parameterization of aquifer properties, results should be interpreted at the system scale. Local values are not intended to represent site-specific conditions, and emphasis should instead be placed on regional spatial patterns and long-term trends.

However, the model is validated using monitoring data from the last 30 years, and constrained by realism criteria, thereby reducing historical uncertainty. While the model results present a wide range of possible historical scenarios, the overall system dynamics remain robust, with most model runs exhibiting consistent patterns. We believe our approach to translating the groundwater basin's hydrogeological conditions into a numerical flow model is an effective strategy given the limited data availability.

4.3 Implications

At present, groundwater resources declines despite groundwater abstractions tending to stabilize. Bierkens & Wada (2019) demonstrated that severe groundwater abstractions can exceed the compensatory effects of river water infiltration, resulting in persistently falling groundwater tables, indicating unsustainable use. Over recent decades, these declines have caused wells to run dry, disproportionately affecting poorer households that cannot afford deeper wells and more expensive submerged pumps. At the same time, rising extraction costs may reduce demand in severely depleted areas and potentially slow further declines (Turner et al., 2019).

Reductions in groundwater exfiltration directly translate into declining surface water fluxes as it reduces baseflow, thereby lowering contributions to downstream Yamuna and Ganges River discharge. Decreasing streamflow across the Indo-Gangetic Basin between 1951 and 2021 was observed by Chuphal and Mishra (2023). Our model confirms this trend, showing decreased groundwater discharge directly to both rivers (Figure 9a and 9d). Although wastewater inputs partly offset declining groundwater contributions, total river discharge continues to decrease due to increasing evapotranspiration from agricultural intensification (Pandeya and Mulligan, 2013) and climate change (Krishnan et al., 2016; Saha and Ghosh, 2020).

Declining baseflow also has implications for surface water quality, because groundwater exfiltration sustains environmental flows and dilutes pollutants. When baseflow is reduced or absent, pollutant concentrations increase. Our findings indicate that municipal wastewater becomes an increasingly dominant component of river discharge, substantially degrading water quality. As emphasized by Forstner et al. (2025), understanding historical system dynamics is essential for setting realistic restoration targets. Without recovery of groundwater tables, baseflow will remain minimal, leaving rivers largely dependent on wastewater and fundamentally altering environmental flows and water quality, impacting both aquatic ecosystems and local communities.

Finally, the shift from draining to infiltrating rivers poses serious risks to groundwater quality, as polluted river water increasingly recharges shallow aquifers used for drinking and irrigation (van Broekhoven et al., 2024). Increased groundwater abstractions and infiltration of contaminated irrigation return flows may accelerate vertical pollutant transport, shorten residence time and limit natural purification processes. The loss of groundwater exfiltration possibly creates a closed-loop system in which pumped groundwater partially evaporates and reinfiltrates, increasing pollutant accumulation within the

https://doi.org/10.5194/egusphere-2026-1584
Preprint. Discussion started: 31 March 2026

aquifer as also hypothesised by Bons (2018). Additionally, municipal return flow, while modest in volume, represents a significant local source of pollution (van Broekhoven et al., 2024). Increased groundwater dependence in the IGB in the future, as indicated by Lutz et al. (2022), will likely increase irrigation abstractions, accelerating groundwater declines (van der Vat et al., 2019). This could also switch the main rivers from draining to infiltrating, further impacting surface water and groundwater quantity and quality.

5 Conclusions

This two-century hindcast study reveals a hydrological regime shift in the Upper Ganges–Yamuna interfluve. The system evolved from a natural (pre-1830) rainfall-dominated equilibrium, to a canal-enhanced recharge phase following construction of the Eastern Yamuna Canal and Upper Ganga Canal, and a contemporary groundwater abstractions dominated state after the Green Revolution (post-1970). Canal leakage initially raised groundwater tables and increased groundwater exfiltration to rivers, but expansion of irrigation abstractions after 1970 lowered groundwater tables below pre-canal conditions and reduced groundwater exfiltration to rivers. Since around 2000, abstraction has exceeded recharge in large parts of the region, with a transition of local rivers from draining to infiltrating conditions and reducing their environmental (base)flows. River surface water is now increasingly dependent on wastewater rather than natural baseflow contributions. This imposes risks like further declines in environmental flows, deterioration of surface water quality due to reduced dilution with clean exfiltrating groundwater, and increased vulnerability of shallow aquifers to contamination through polluted river water infiltration. Without structural reductions in irrigation abstractions or substantial recharge enhancement, recovery of pre-1970 groundwater–surface water dynamics appears unlikely.

Appendix A: Quantifying groundwater abstractions and recharge temporally and spatially

This appendix describes the methods used to construct spatially and temporally explicit datasets for all groundwater abstraction and recharge components used as model forcings. Because direct observations of these variables are limited, multiple datasets were combined with literature-based parameters and informed assumptions to derive consistent estimates for each component across the simulation period. All spatial datasets were reprojected to the coordinate reference system WGS 84 / UTM zone 43N (EPSG:32643) to ensure consistency with the model grid. Vector datasets were rasterized to the model grid resolution. Raster datasets with differing spatial resolutions were resampled to the model grid by linear interpolation when downscaling or by averaging the values of underlying cells when upscaling, unless otherwise specified. Missing values were filled using nearest-neighbour interpolation. For each groundwater abstraction and recharge component spatio-temporal datasets were generated for every model cell and time step. The following subsections describe the data sources, assumptions, and processing steps used to quantify each component.

https://doi.org/10.5194/egusphere-2026-1584
Preprint. Discussion started: 31 March 2026

A.1 Irrigation groundwater demand

Irrigation groundwater demand was derived by estimating the amount of groundwater-irrigated hectares per cell multiplied by average yearly irrigation demand per hectare. The current spatial distribution of groundwater-irrigated agriculture was determined by resampling the Copernicus Global Land Cover map (Buchhorn et al., 2020) to calculate total agriculture per cell. This was adjusted using the ratio of total agriculture to groundwater-irrigated agriculture, based on 2011 census data (Government of India, 2011). A logistic growth curve (parameters: L=283 km³/year, k=0.0819, t0=1987) was constructed using national Indian groundwater withdrawal trends from the United Nations World Water Development Report 2022 (UN Water, 2022). The curve was normalized to the 2011 census reference year and fitted to hindcast groundwater withdrawal for irrigated agriculture over time. For the average yearly water demand per hectare, literature-based crop coefficients were applied. Crop water demand was calculated as potential evapotranspiration (ET) multiplied by the crop coefficient. Irrigation demand was then derived by adjusting for return flow and subtracting precipitation. District-level crop distribution was sourced from the INTACH report (INTACH, 2017), with sugarcane (35.8%), wheat (30.4%), rice (9.5%), and other crops (25.4%) as the primary crops. Monthly crop coefficients were obtained from IWMI Research Report 140 (Cai et al., 2010). By combining district-wise crop data with crop coefficients, monthly crop coefficients per district were derived. Monthly irrigation water demand was calculated by multiplying potential evapotranspiration (PET) from the CRU TS dataset (Harris et al., 2020) by the district-level crop coefficient and subtracting precipitation (CRU TS). Only positive values were retained, as irrigation demand cannot be negative.

A.2 Municipal groundwater demand

Regarding municipal groundwater demand we assumed all domestic water was sourced from groundwater. Demand was calculated by multiplying the number of inhabitants per cell by per capita water usage estimates from literature. Population data from WorldPop (Bondarenko et al., 2025) was used to get the spatial distribution of current inhabitants. The HYDE 3.2 population count dataset (Klein Goldewijk et al., 2017) was used to hindcast historical population trends spatially explicit with 2017 as the baseline. Per capita domestic water usage was taken from Joseph et al. (2021) for the years 1975 to 2015. This water usage has been linearly extrapolated backwards to 1800 where daily 25 litre per capita was assumed.

A.3 Industrial groundwater demand

Industrial groundwater demand was estimated using a dataset of industrial locations and their water discharge for a specific year (Uttar Pradesh Pollution Control Board, n.d.). We assumed all industrial water was sourced from groundwater and applied a logistic trendline derived from national groundwater withdrawal rates (UN Water, 2022) to hindcast demand, assuming industrial locations remained constant over time.

https://doi.org/10.5194/egusphere-2026-1584
Preprint. Discussion started: 31 March 2026

A.4 Rainfall recharge

Rainfall recharge was derived from the CRU TS dataset (1901–2024) (Harris et al., 2020), resampled to match our model grid. Recharge was calculated as the sum of monthly rainfall minus an estimated 2% for surface runoff and minus monthly potential evapotranspiration, with only non-negative values considered. For the period before 1900, the long-term rainfall recharge average was used due to data limitations, assuming no significant climate shifts.

A.5 Canal leakage recharge

Canal leakage recharge was estimated by multiplying the canal area per cell by a leakage factor. Canal area per cell was derived from the India-WRIS dataset (India-WRIS, n.d.), which provides canal locations, types, and names. Canal width was assumed to vary between 5 m and 100 m depending on canal type. The leakage factor was based on Raza et al. (2013), who reported seepage losses of 0.32 L s^{-1} per 100 m of unlined canal. Assuming an average canal width of 25 m in that study, this corresponds to an approximate leakage rate of 11 mm day^{-1} m^{-2} of canal area. Construction dates for individual canal sections were estimated from literature sources and used for hindcasting. Small-scale canal systems in the Indo-Gangetic Basin (IGB) date back to 16th century under Mughal rule (Jain et al., 2022). However, their contribution to regional groundwater recharge was like minor compared with the extensive canal networks developed under British rule. We therefore quantified canal leakage only from 1830 (Eastern Yamuna Canal) and 1856 (Upper Ganga Canal), periods when such infrastructure began to significantly influence the groundwater balance and groundwater-surface water interactions.

A.6 Irrigation return flow recharge

Irrigation return flow recharge was estimated by applying a groundwater return flow factor of 0.162 to the total irrigation demand. This factor is based on Gupta and Deshpande (2004, as cited in van der Vat, 2018) who found an efficiency factor of 0.7 and a return flow percentage to groundwater of 54% of total gross demand not transpired by the crop. Flood irrigation, the predominant irrigation method in the Indo-Gangetic Basin (IGB), leads to considerable evaporation losses but also generates substantial return flows to the groundwater system. Total irrigation demand consists of both groundwater and canal water demand. It was estimated using the same approach as the groundwater irrigation demand calculation; however, instead of the groundwater-irrigated ratio, the total irrigated ratio derived from the 2011 census data published by the (Government of India, 2011) was applied. Hindcasting was performed using total irrigated area from HYDE 3.2 (Klein Goldewijk et al., 2017), averaged across the entire Indo-Gangetic Basin (IGB) at each time step.

A.7 Municipal return flow recharge

Municipal return flow recharge was calculated by multiplying municipal demand by a leakage factor. The leakage factor varies depending on the distance to rivers. Municipal wastewater was assumed to discharge to rivers within 2.5 km and to ponds beyond that distance, with different infiltration rates applied accordingly. The wastewater discharge to rivers is assumed to

https://doi.org/10.5194/egusphere-2026-1584
Preprint. Discussion started: 31 March 2026

have a leakage factor of 0.10. The wastewater discharged to pond is assumed to partly evaporate and partly infiltrate (factor 0.65).

Code and data availability

All datasets and python code used in this study are available at Zenodo: https://doi.org/10.5281/zenodo.19131621 (van Broekhoven, 2026).

Author contributions

F.J.G. van Broekhoven: Writing – original draft, Validation, Software, Methodology, Investigation, Formal analysis, Conceptualization. S.C. Dekker: Writing – review & editing, Supervision, Methodology, Funding acquisition, Conceptualization. J. Griffioen: Writing – review & editing, Supervision, Methodology, Conceptualization. A. Bhagwat: Writing – review & editing, Investigation. P.P. Schot: Writing – review & editing, Supervision, Methodology, Funding acquisition, Conceptualization.

Competing interests

The authors declare that they have no conflict of interest.

Disclaimer

Copernicus Publications remains neutral with regard to jurisdictional claims made in the text, published maps, institutional affiliations, or any other geographical representation in this paper. While Copernicus Publications makes every effort to include appropriate place names, the final responsibility lies with the authors. Views expressed in the text are those of the authors and do not necessarily reflect the views of the publisher.

Acknowledgements

Authors acknowledge the support of the Director of National Institute of Hydrology, Roorkee (NIH), of Raul Mendoza and Thomson Chow both from Wageningen University and Research for model input collection, and Martijn van Leer from Utrecht University and TNO Geological Survey of the Netherlands for assisting with MODFLOW 6 Flopy scripting. AI tools were used in the preparation of this manuscript to improve readability, including spelling, grammar, and sentence structure, and in generating parts of Python code, including docstrings and documentation. All outputs were reviewed and revised by the authors as needed.

https://doi.org/10.5194/egusphere-2026-1584
Preprint. Discussion started: 31 March 2026

Financial support

This work was part of the Cleaning the Ganga, Agri-Water project, jointly funded by Dutch Research Council (NWO), through the Merian Fund [Grant number: 482.20.309], and the Indian Department of Science and Technology (DST).

References

Alam, F. and Umar, R.: Groundwater flow modelling of Hindon-Yamuna interfluve region, Western Uttar Pradesh, J. Geol. Soc. India, 82, 80–90, https://doi.org/10.1007/s12594-013-0113-8, 2013.

Bakker, M., Post, V., Langevin, C. D., Hughes, J. D., White, J. T., Starn, J. J., and Fienen, M. N.: Scripting MODFLOW Model Development Using Python and FloPy, Groundwater, 54, 733–739, https://doi.org/10.1111/gwat.12413, 2016.

Ballio, F. and Guadagnini, A.: Convergence assessment of numerical Monte Carlo simulations in groundwater hydrology, Water Resour. Res., 40, https://doi.org/10.1029/2003WR002876, 2004.

Bekesi, G. and McConchie, J.: Groundwater recharge modelling using the Monte Carlo technique, Manawatu region, New Zealand, J. Hydrol., 224, 137–148, https://doi.org/10.1016/S0022-1694(99)00128-6, 1999.

Bierkens, M. F. P. and Wada, Y.: Non-renewable groundwater use and groundwater depletion: a review, Environ. Res. Lett., 14, 063002, https://doi.org/10.1088/1748-9326/ab1a5f, 2019.

Bondarenko, M., Priyatikanto, R., Tejedor Garavito, N., Zhang, W., McKeen, T., Cunningham, A., Woods, T., Hilton, J., Cihan, D., Nosatiuk, B., Brinkhoff, T., Tatem, A., and Sorichetta, A.: Constrained estimates of 2015-2030 total number of people per grid square at a resolution of 30 arc (approximately 1km at the equator) R2025A version v1., https://doi.org/10.5258/SOTON/WP00840, 2025.

Bons, K.: Ganga River Basin Planning Assessment Report. Main volume and Appendices., Deltares with AECOM and FutureWater, 2018.

Bonsor, H. C., MacDonald, A. M., Ahmed, K. M., Burgess, W. G., Basharat, M., Calow, R. C., Dixit, A., Foster, S. S. D., Gopal, K., Lapworth, D. J., Moench, M., Mukherjee, A., Rao, M. S., Shamsudduha, M., Smith, L., Taylor, R. G., Tucker, J., van Steenbergen, F., Yadav, S. K., and Zahid, A.: Hydrogeological typologies of the Indo-Gangetic basin alluvial aquifer, South Asia, Hydrogeol. J., 25, 1377–1406, https://doi.org/10.1007/s10040-017-1550-z, 2017.

van Broekhoven, F. J. G.: Data and code: Changes in groundwater-surface water interactions following two centuries of irrigation practices and groundwater use in the Upper Ganges-Yamuna interfluve, North India. Zenodo [data set], https://doi.org/10.5281/zenodo.19131621, 2026.

https://doi.org/10.5194/egusphere-2026-1584
Preprint. Discussion started: 31 March 2026

van Broekhoven, F. J. G., Griffioen, J., Dekker, S. C., Sharma, M. K., Bhagwat, A., and Schot, P. P.: Linking recharge water sources to groundwater composition in the Hindon subbasin of the Ganges River, India, Sci. Total Environ., 954, 176399, https://doi.org/10.1016/j.scitotenv.2024.176399, 2024.

Buchhorn, M., Smets, B., Bertels, L., Roo, B. D., Lesiv, M., Tsendbazar, N.-E., Herold, M., and Fritz, S.: Copernicus Global Land Service: Land Cover 100m: collection 3: epoch 2015: Globe, https://doi.org/10.5281/zenodo.3939038, 2020.

Cai, X., Sharma, B. R., Matin, M. A., Sharma, D., and Gunasinghe, S.: An assessment of crop water productivity in the Indus and Ganges River Basins: current status and scope for improvement, International Water Management Institute, https://doi.org/10.5337/2010.232, 2010.

Chuphal, D. S. and Mishra, V.: Hydrological model-based streamflow reconstruction for Indian sub-continental river basins, 1951–2021, Sci. Data, 10, 717, https://doi.org/10.1038/s41597-023-02618-w, 2023.

Drew, G.: Transformation and Resistance on the Upper Ganga: The Ongoing Legacy of British Canal Irrigation, South Asia J. South Asian Stud., 37, 670–683, https://doi.org/10.1080/00856401.2014.966896, 2014.

Forstner, T. A., Morgan, L. K., Moore, C., and Kitlasten, W.: Leveraging the past to inform groundwater futures: A review of data archives, reconstruction approaches and opportunities for groundwater hindcasting applications, J. Hydrol., 656, 132924, https://doi.org/10.1016/j.jhydrol.2025.132924, 2025.

Gleeson, T., Wada, Y., Bierkens, M. F. P., and van Beek, L. P. H.: Water balance of global aquifers revealed by groundwater footprint, Nature, 488, 197–200, https://doi.org/10.1038/nature11295, 2012.

Government of India: Census of India 2011, 2011.

de Graaf, I. E. M., van Beek, R. L. P. H., Gleeson, T., Moosdorf, N., Schmitz, O., Sutanudjaja, E. H., and Bierkens, M. F. P.: A global-scale two-layer transient groundwater model: Development and application to groundwater depletion, Adv. Water Resour., 102, 53–67, https://doi.org/10.1016/j.advwatres.2017.01.011, 2017.

de Graaf, I. E. M., Gleeson, T., (Rens) van Beek, L. P. H., Sutanudjaja, E. H., and Bierkens, M. F. P.: Environmental flow limits to global groundwater pumping, Nature, 574, 90–94, https://doi.org/10.1038/s41586-019-1594-4, 2019.

Harris, I., Osborn, T. J., Jones, P., and Lister, D.: Version 4 of the CRU TS monthly high-resolution gridded multivariate climate dataset, Sci. Data, 7, 109, https://doi.org/10.1038/s41597-020-0453-3, 2020.

India-WRIS: Water Resource Information Systems of India, n.d.

INTACH: Reviving Hindon River: A Basin Approach, Natural Heritage Division, INTACH, New Delhi, New Delhi, 2017.

Irrigation and Water Resources Department: Yamuna, Ministry of Jal Shakti, Government of Uttar Pradesh, Uttar Pradesh, India, n.d.

Jadav, K. and Yadav, B.: The Hindon River basin crisis: Anthropogenic and climatic impacts on groundwater depletion and public health risks, J. Hydrol. Reg. Stud., 61, 102661, https://doi.org/10.1016/j.ejrh.2025.102661, 2025.

Jain, C. K. and Sharma, M. K.: Heavy Metal Transport in the Hindon River Basin, India, Environ. Monit. Assess., 112, 255–270, https://doi.org/10.1007/s10661-006-1706-0, 2006.

https://doi.org/10.5194/egusphere-2026-1584
Preprint. Discussion started: 31 March 2026

Jain, S., Sharma, A., and Mujumdar, P. P.: Evolution of Water Management Practices in India, in: Riverine Systems: Understanding the Hydrological, Hydrosocial and Hydro-heritage Dynamics, edited by: Mukherjee, A., Springer International Publishing, Cham, 325–349, https://doi.org/10.1007/978-3-030-87067-6_18, 2022.

Joseph, N., Ryu, D., Malano, H. M., George, B., and Sudheer, K. P.: Estimation of state-wide and monthly domestic water use in India from 1975 to 2015, Urban Water J., 18, 421–432, https://doi.org/10.1080/1573062X.2021.1893362, 2021.

Joshi, S. K., Gupta, S., Sinha, R., Logan Densmore, A., Prakash Rai, S., Shekhar, S., Mason, P. J., and Dijk, W. M. van: Strongly heterogeneous patterns of groundwater depletion in Northwestern India, J. Hydrol., 598, 126492, https://doi.org/10.1016/j.jhydrol.2021.126492, 2021.

Kahe, M. S., Javadi, S., Roozbahani, A., and Mohammadi, K.: Parametric uncertainty analysis on hydrodynamic coefficients in groundwater numerical models using Monte Carlo method and RPEM, Environ. Dev. Sustain., 23, 11583–11606, https://doi.org/10.1007/s10668-020-01128-8, 2021.

Klein Goldewijk, K., Beusen, A., Doelman, J., and Stehfest, E.: Anthropogenic land use estimates for the Holocene – HYDE 3.2, Earth Syst. Sci. Data, 9, 927–953, https://doi.org/10.5194/essd-9-927-2017, 2017.

Krishnan, R., Sabin, T. P., Vellore, R., Mujumdar, M., Sanjay, J., Goswami, B. N., Hourdin, F., Dufresne, J.-L., and Terray, P.: Deciphering the desiccation trend of the South Asian monsoon hydroclimate in a warming world, Clim. Dyn., 47, 1007–1027, https://doi.org/10.1007/s00382-015-2886-5, 2016.

Langevin, C., Hughes, J., Banta, E., Niswonger, R., Panday, S., and Provost, A.: Documentation for the MODFLOW 6 Groundwater Flow Model, Reston, VA, https://doi.org/10.3133/tm6A55, 2017.

Lehner, B., Verdin, K., and Jarvis, A.: New Global Hydrography Derived From Spaceborne Elevation Data, Eos Trans. Am. Geophys. Union, 89, 93–94, https://doi.org/10.1029/2008EO100001, 2008.

Lewis, H.: Hindon River: Gasping for breath: A Paper on River Pollution, 2007.

Lutz, A. F., Immerzeel, W. W., Siderius, C., Wijngaard, R. R., Nepal, S., Shrestha, A. B., Wester, P., and Biemans, H.: South Asian agriculture increasingly dependent on meltwater and groundwater, Nat. Clim. Change, 12, 566–573, https://doi.org/10.1038/s41558-022-01355-z, 2022.

MacAllister, D. J., Krishan, G., Basharat, M., Cuba, D., and MacDonald, A. M.: A century of groundwater accumulation in Pakistan and northwest India, Nat. Geosci., 15, 390–396, https://doi.org/10.1038/s41561-022-00926-1, 2022.

Maheswaran, R., Khosa, R., Gosain, A. K., Lahari, S., Sinha, S. K., Chahar, B. R., and Dhanya, C. T.: Regional scale groundwater modelling study for Ganga River basin, J. Hydrol., 541, 727–741, https://doi.org/10.1016/j.jhydrol.2016.07.029, 2016.

Marinelli, B. P. P., Mohan, C., Gleeson, T., Ludwig, F., and de Graaf, I. E. M.: Comparing Global Violations of Environmentally Critical Groundwater Discharge Thresholds, Water Resour. Res., 60, e2024WR037519, https://doi.org/10.1029/2024WR037519, 2024.

https://doi.org/10.5194/egusphere-2026-1584
Preprint. Discussion started: 31 March 2026

Mendoza, R., Verseveld, W. J. van, Weiland, F. S., Bhagwat, A., Seijger, C., and Weerts, A. H.: Assessing hydrological model representation of irrigation and subsurface flow in a heavily anthropogenic influenced catchment, https://doi.org/10.22541/essoar.177006135.59709410/v1, 2 February 2026.

Mourad, R., Schoups, G., Bastiaanssen, W., and Kumar, D. N.: Expert-based prior uncertainty analysis of gridded water balance components: Application to the irrigated Hindon River Basin, India, J. Hydrol. Reg. Stud., 55, 101935, https://doi.org/10.1016/j.ejrh.2024.101935, 2024.

Panda, D. K., Ambast, S. K., and Shamsudduha, M.: Groundwater depletion in northern India: Impacts of the sub-regional anthropogenic land-use, socio-politics and changing climate, Hydrol. Process., 35, e14003, https://doi.org/10.1002/hyp.14003, 2021.

Pandeya, B. and Mulligan, M.: Modelling crop evapotranspiration and potential impacts on future water availability in the Indo-Gangetic Basin, Agric. Water Manag., 129, 163–172, https://doi.org/10.1016/j.agwat.2013.07.019, 2013.

Pingali, P. L.: Green Revolution: Impacts, limits, and the path ahead, Proc. Natl. Acad. Sci., 109, 12302–12308, https://doi.org/10.1073/pnas.0912953109, 2012.

Raza, A., Latif, M., and Shakir, A. S.: Long-Term Effectiveness of Lining Tertiary Canals in the Indus Basin of Pakistan, Irrig. Drain., 62, 16–24, https://doi.org/10.1002/ird.1714, 2013.

Rodell, M., Velicogna, I., and Famiglietti, J. S.: Satellite-based estimates of groundwater depletion in India, Nature, 460, 999–1002, https://doi.org/10.1038/nature08238, 2009.

Saha, A. and Ghosh, S.: Relative Impacts of Projected Climate and Land Use Changes on Terrestrial Water Balance: A Case Study on Ganga River Basin, Front. Water, 2, https://doi.org/10.3389/frwa.2020.00012, 2020.

Scanlon, B. R., Fakhreddine, S., Rateb, A., De Graaf, I., Famiglietti, J., Gleeson, T., Grafton, R. Q., Jobbagy, E., Kebede, S., Kolusu, S. R., Konikow, L. F., Long, D., Mekonnen, M., Schmied, H. M., Mukherjee, A., MacDonald, A., Reedy, R. C., Shamsudduha, M., Simmons, C. T., Sun, A., Taylor, R. G., Villholth, K. G., Vörösmarty, C. J., and Zheng, C.: Global water resources and the role of groundwater in a resilient water future, Nat. Rev. Earth Environ., 4, 87–101, https://doi.org/10.1038/s43017-022-00378-6, 2023.

Swarnkar, S., Mujumdar, P., and Sinha, R.: Modified hydrologic regime of upper Ganga basin induced by natural and anthropogenic stressors, Sci. Rep., 11, 19491, https://doi.org/10.1038/s41598-021-98827-7, 2021.

Turner, S. W. D., Hejazi, M., Yonkofski, C., Kim, S. H., and Kyle, P.: Influence of Groundwater Extraction Costs and Resource Depletion Limits on Simulated Global Nonrenewable Water Withdrawals Over the Twenty-First Century, Earths Future, 7, 123–135, https://doi.org/10.1029/2018EF001105, 2019.

Umar, R., Khan, M. M. A., Ahmed, I., and Ahmed, S.: Implications of Kali-Hindon inter-stream aquifer water balance for groundwater management in western Uttar Pradesh, J. Earth Syst. Sci., 117, 69–78, https://doi.org/10.1007/s12040-008-0014-1, 2008.

UN Water (Ed.): Groundwater making the invisible visible, UNESCO, Paris, 225 pp., 2022.

https://doi.org/10.5194/egusphere-2026-1584
Preprint. Discussion started: 31 March 2026

Uttar Pradesh Pollution Control Board: Action Plan for Restoration of Polluted Stretch of River Hindon from District Saharanpur to District Ghaziabad, Uttar Pradesh Pollution Control Board, Lucknow, Uttar Pradesh, India, n.d.

Van Dijk, W. M., Densmore, A. L., Jackson, C. R., Mackay, J. D., Joshi, S. K., Sinha, R., Shekhar, S., and Gupta, S.: Spatial variation of groundwater response to multiple drivers in a depleting alluvial aquifer system, northwestern India, Prog. Phys. Geogr. Earth Environ., 44, 94–119, https://doi.org/10.1177/0309133319871941, 2020.

van der Vat, M.: Ganga River Basin Model and Information System, Report and Documentation. Main volume and Appendices., Deltares with AECOM and FutureWater for the World Bank and the Government of India, 2018.

van der Vat, M., Boderie, P., Bons, K., Hegnauer, M., Hendriksen, G., van Oorschot, M., Ottow, B., Roelofsen, F., Sankhua, R. N., Sinha, S. K., Warren, A., and Young, W.: Participatory Modelling of Surface and Groundwater to Support Strategic Planning in the Ganga Basin in India, Water, 11, 2443, https://doi.org/10.3390/w11122443, 2019.

de Vries, J. J.: Seasonal expansion and contraction of stream networks in shallow groundwater systems, J. Hydrol., 170, 15–26, https://doi.org/10.1016/0022-1694(95)02684-H, 1995.